Electronic Supplementary Material (ESI) for Nanoscale.

SUPPORTING INFORMATION

Solvent-driven chirality for luminescent self- assembled structures: experiments and theory

Charles Lochenie, Alberto Insuasty, Tommaso Battisti, Luca Pesce, Andrea Gardin, Claudio Perego, Mike Dentinger, Di Wang, Giovanni M. Pavan*, Alessandro Aliprandi* and Luisa De Cola*

Synthesis of the ligand and of the complex:

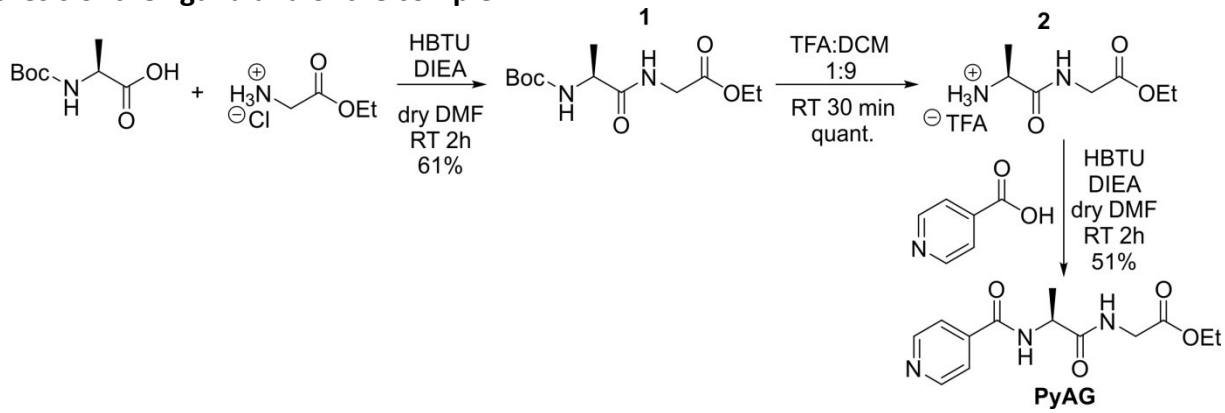

Figure S1: Reaction Scheme for the synthesis of **PyAG**

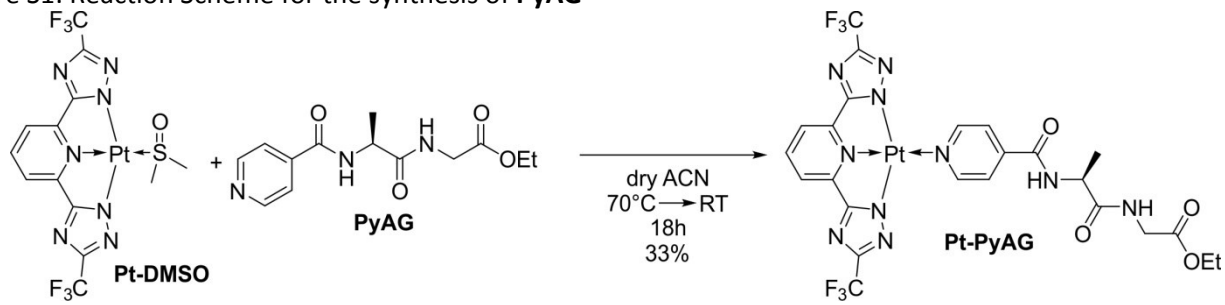

Figure S2: Reaction Scheme for the synthesis of **Pt-PyAG**

Characterization of the compounds:

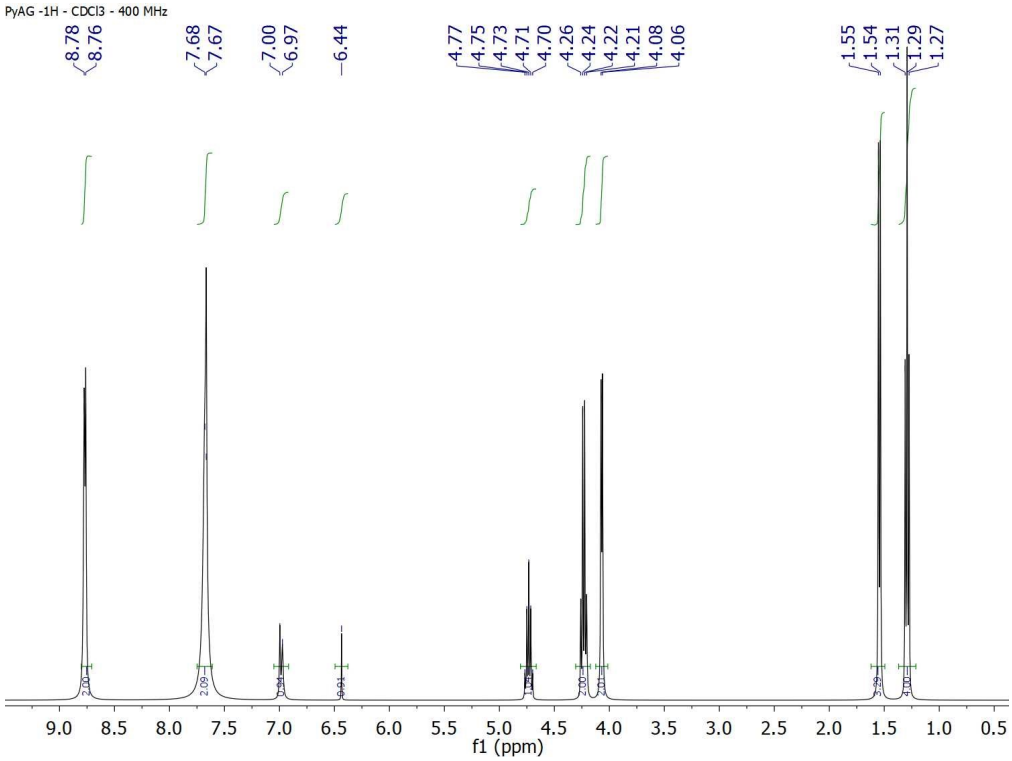

Figure S3: ^{1}H-NMR of ligand **PyAG** ($CDCl_3$, 400 MHz).

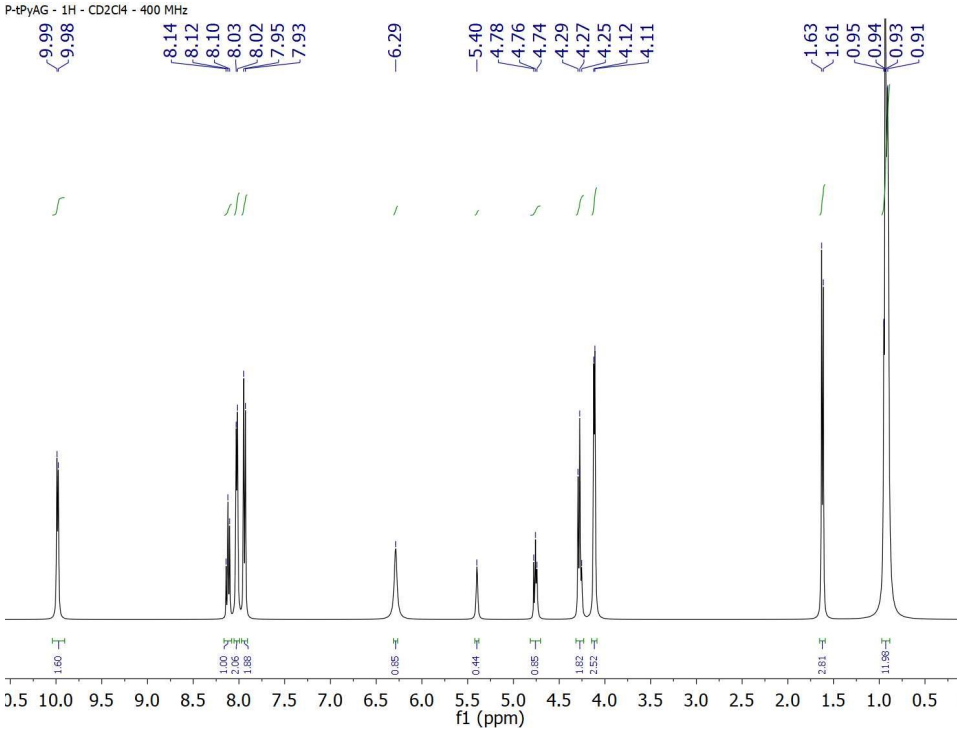

Figure S4: ^{1}H-NMR of complex **Pt-PyAG** (CD_2Cl_4, 400 MHz).

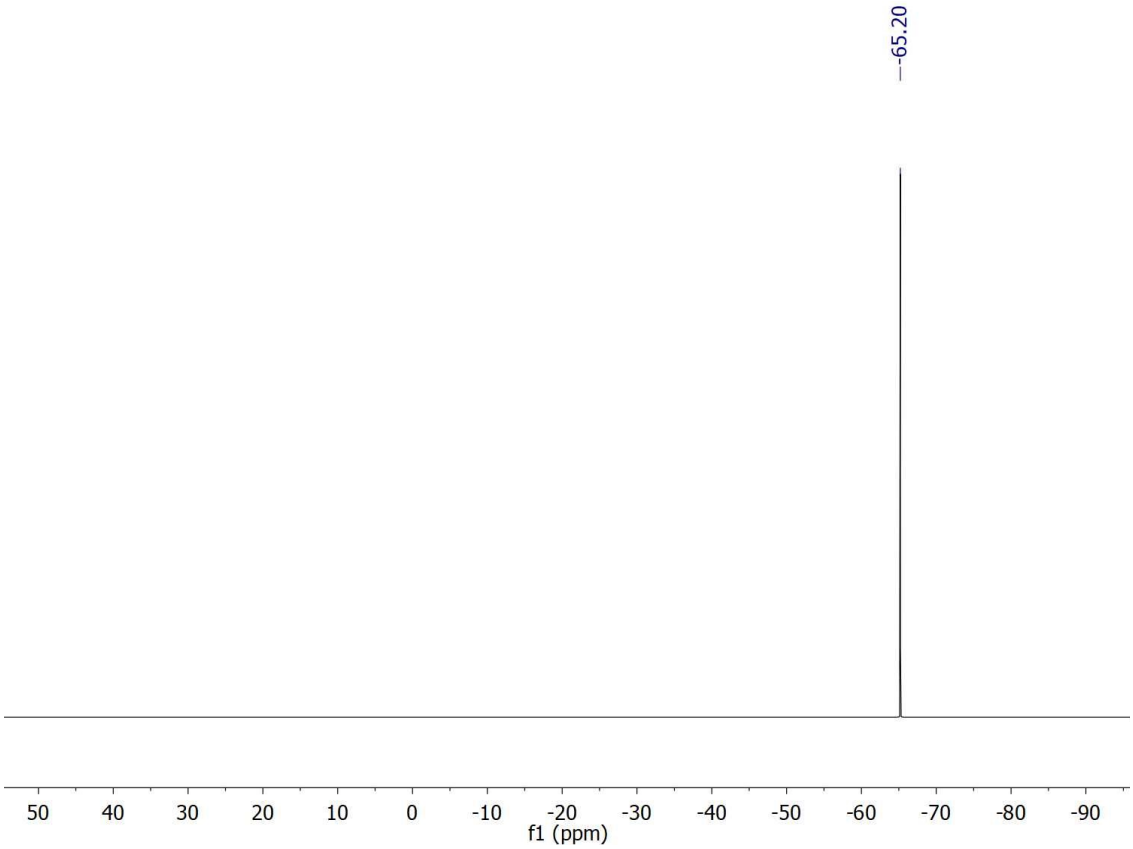

Figure S5: ^{19}F-NMR of complex **Pt-PyAG** (CD_2Cl_4, 400 MHz).

Self-assembly of the complex in different solvents:

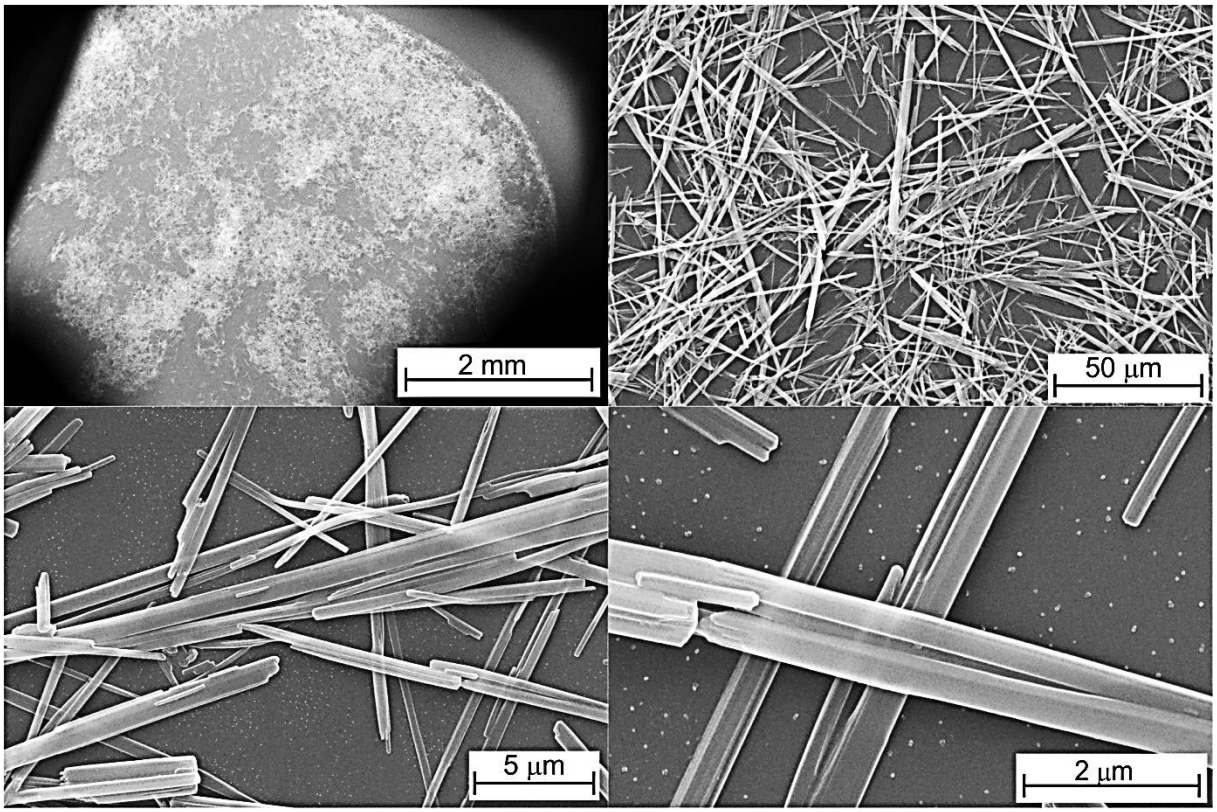

Figure S6: SEM images of the ribbon-like fibers of **Pt-PyAG** in ACN.

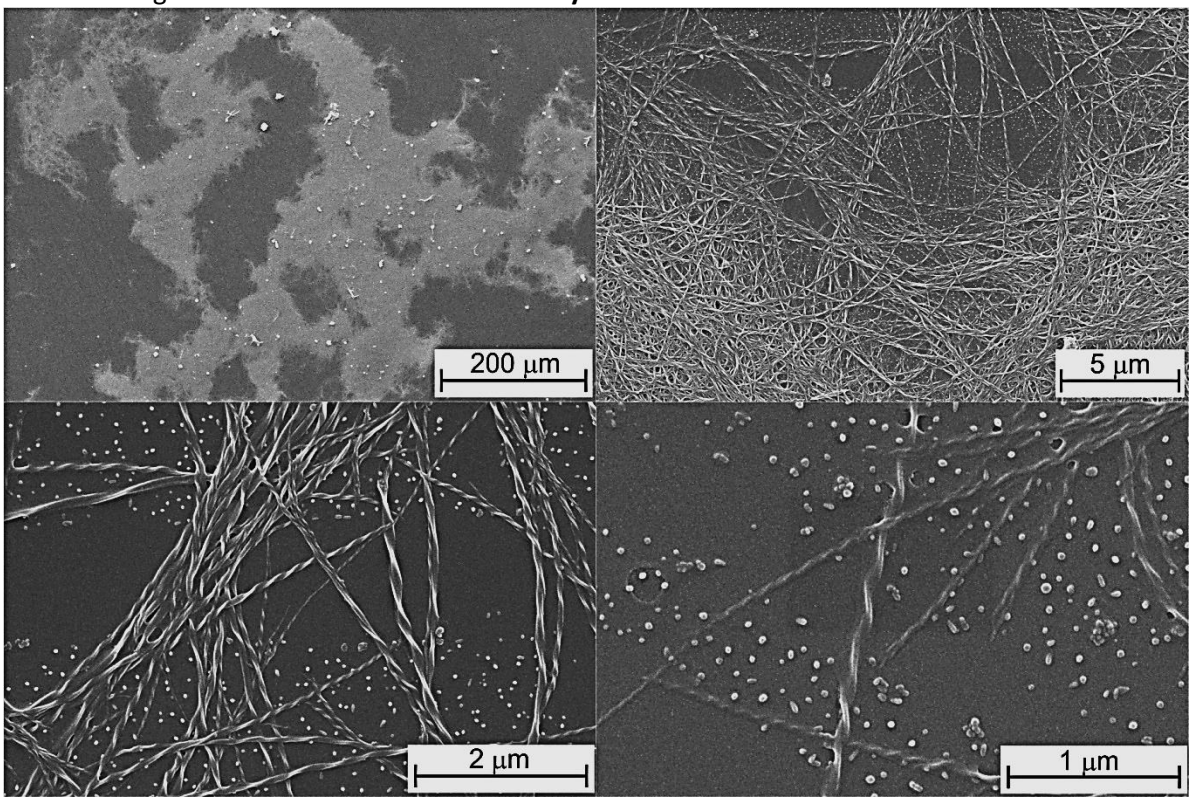

Figure S7: SEM images of the twisted fibers of **Pt-PyAG** in TCE.

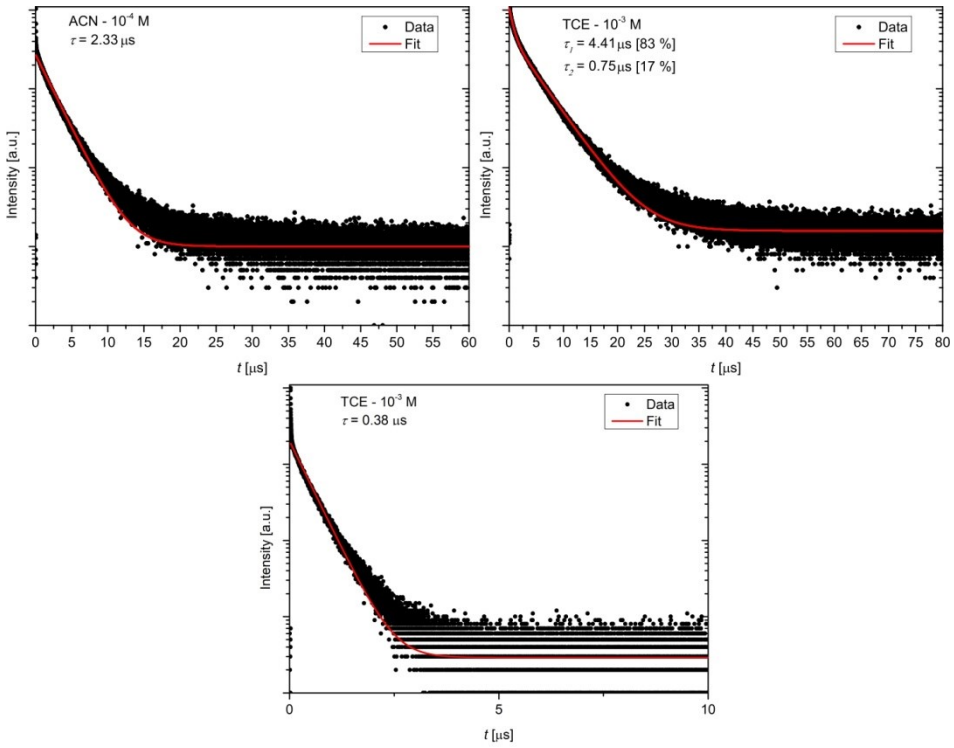

Figure S8: Excited-state lifetime decays of **Pt-PyAG** in ACN (10^{-4} M) and TCE (10^{-3} M) (λ_{exc} = 375 nm; λ_{em} = 465 nm) (top) ; and of Pt-PyAG in TCE (10^{-3} M, λ_{exc} = 375 nm; λ_{em} = 575 nm) (bottom). Decays were fitted with an exponential using a tailfit function.

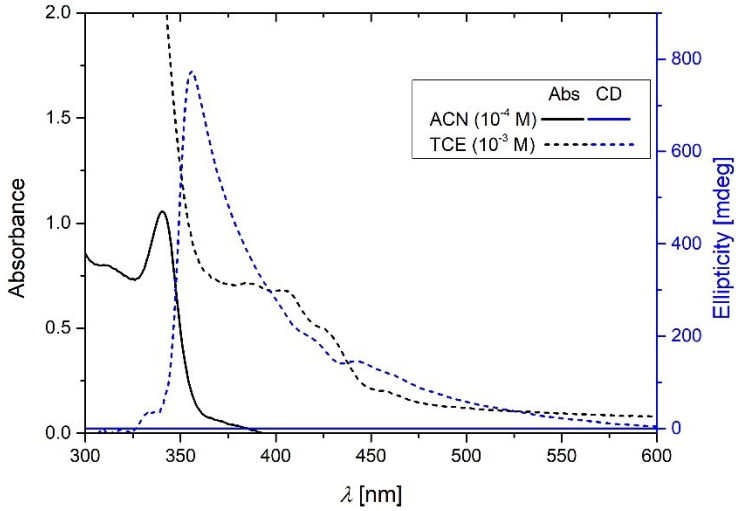

Figure S9: Absorption and CD spectra of **Pt-PyAG** in ACN (10^{-4} M) and TCE (10^{-3} M).

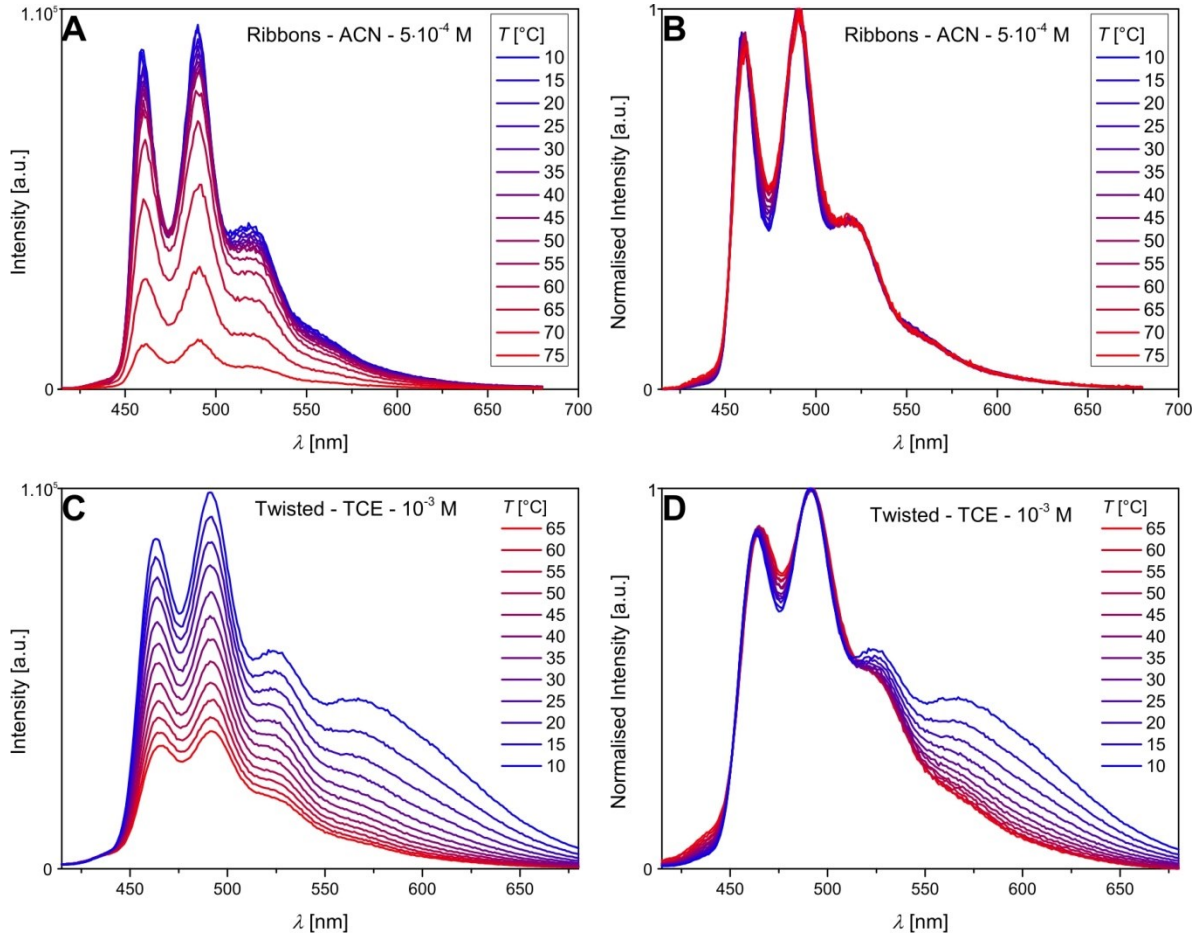

Figure S10: Temperature-dependent emission spectra and normalized spectra of the ribbons (A&B) and the twisted fibers (C&D) λ_{exc} = 350 nm).

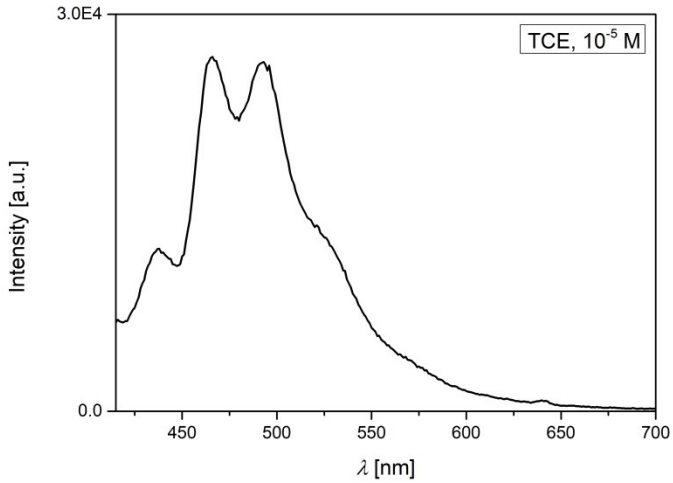

Figure S11: Emission spectrum of the molecularly dissolved Pt-PyAG in TCE at 10^{-5} M (λ_{exc} = 350 nm) (very weak emission).

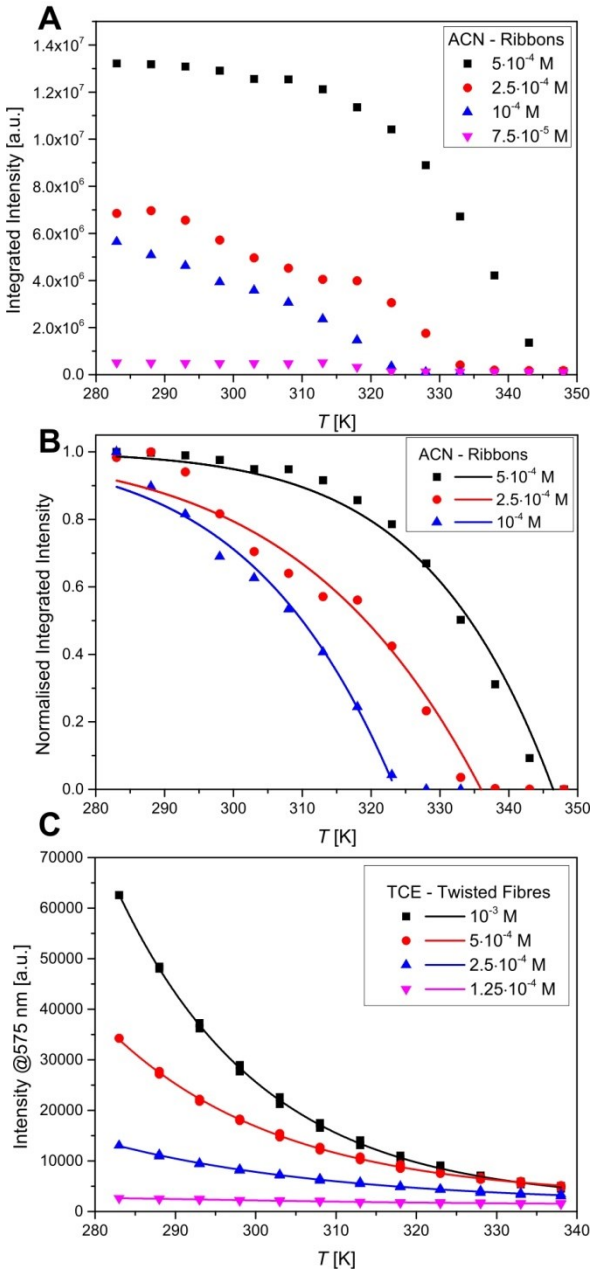

Figure S12. A. Integrated emission intensity vs. temperature for the ribbons at different concentrations; B. Normalized emission intensity vs. temperature (symbols) with the exponential fits (line) for the nanoribbons; C. Integrated emission intensity vs. temperature (symbols) with the sigmoidal fits (line) for the twisted fibers.

The fitting of the data presented in Figure S11B was performed using the following equation:

$$y = 1 - a * exp(-\frac{b}{x})$$

The fitting of the data presented in Figure S11C was performed using the following equation:

$$y = A2 + (A1 - A2)/(1 + \frac{\exp(x - x0)}{dx})$$

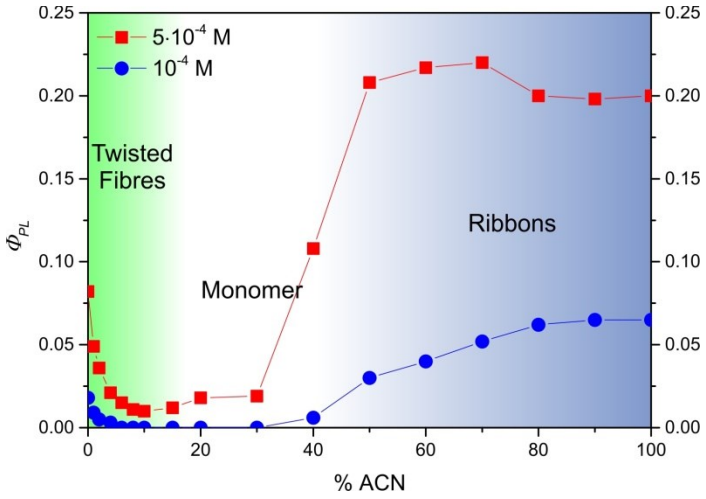

Figure S13. Quantum yield (Φ_{exc} = 350 nm) vs. solvent composition (TCE/ACN) at different concentrations.

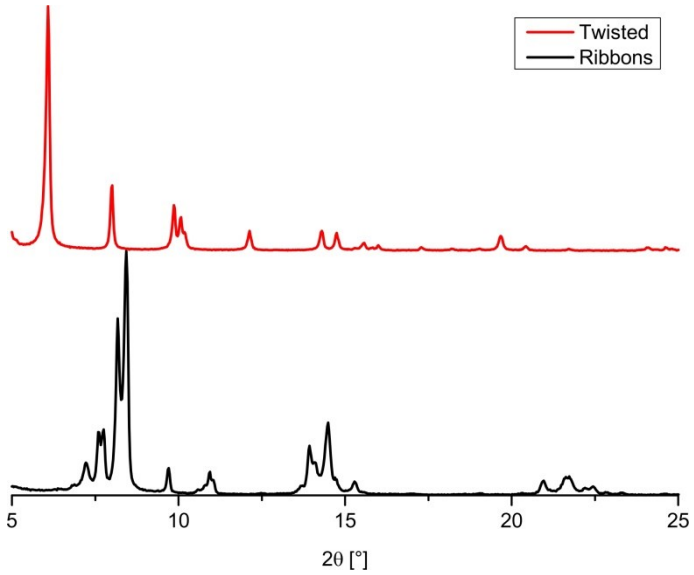

Figure S14. Powder X-ray diffraction patterns of the ribbons (black line) and the twisted fibers (red) of **Pt-PyAG**.

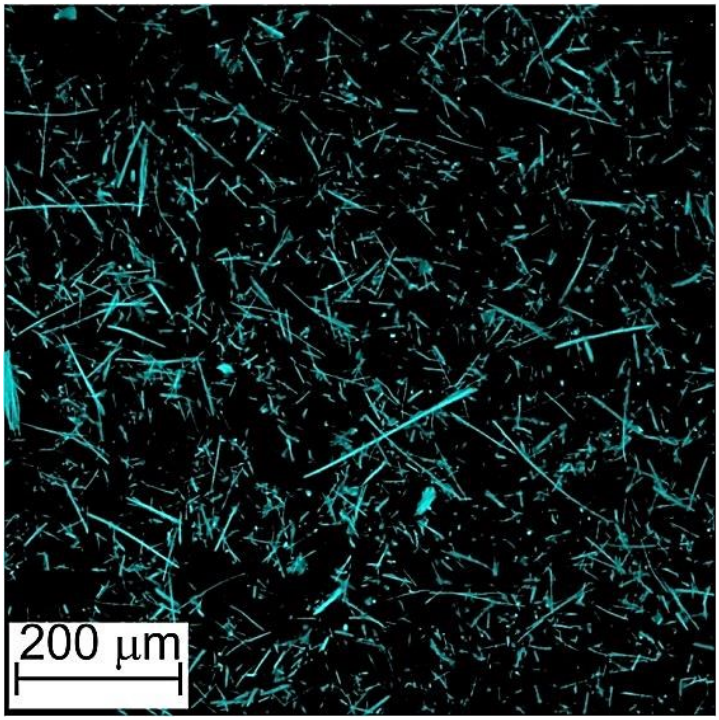

Figure S15. Confocal fluorescence microscopy image of the nanoribbons in lambda mode (λ_{exc} = 405 nm).

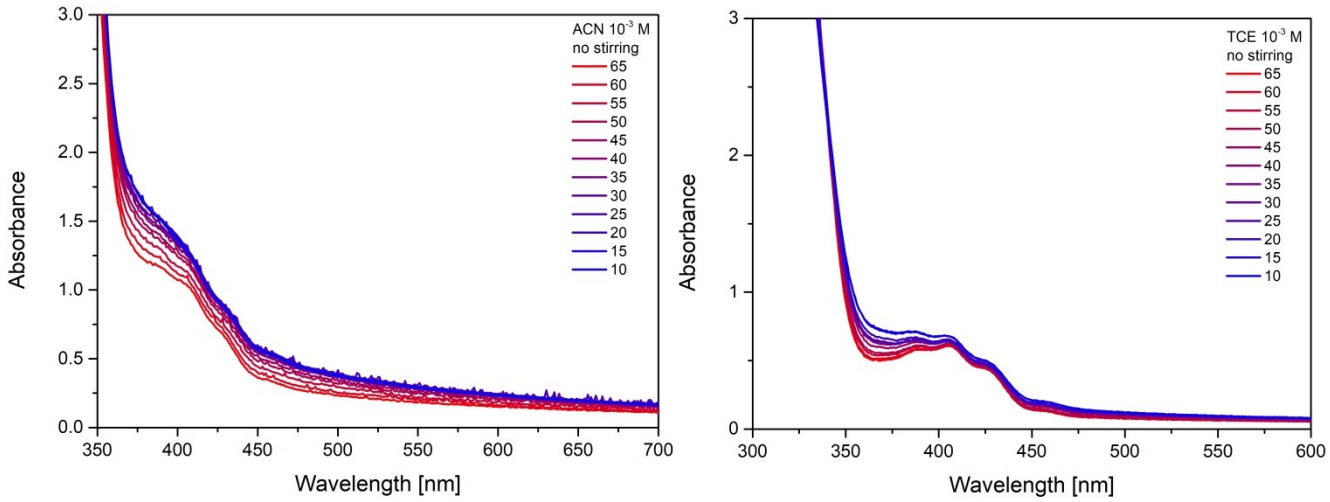

Figure S16. Temperature-dependent absorption spectra of Pt-PyAG in ACN (top) and TCE (bottom)

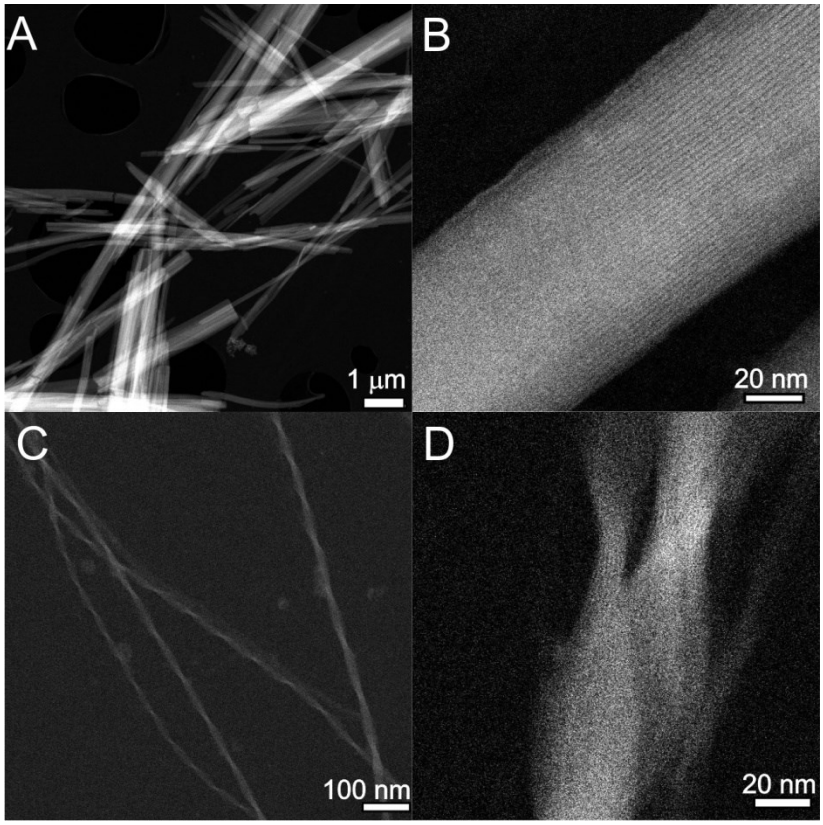

Figure S17. ADF-STEM images of the nanoribbons (A&B) and the twisted fibers (C&D)

Extended details on AA and CG models parametrization

Details of all atom models parametrization

The computational All-Atom (AA) model of Pt-PyAG was parametrized according to the general AMBER force field (GAFF) [1], by using the AMBERtools 17 [2], while the missing parameters related to the atoms coordinating to the Pt atom were obtained following the procedure of the Metal Center Parameter Builder (MCPB) [3]. Here the system was considered neutral and the wavefunction was set in its singlet state. After running a preliminary geometrical optimization using the PM6 semi empirical method[4,5] the models were optimized at the B3LYP level of theory [6], by using 6-31G* basis set (BS) for the elements of the first three periods of the periodic table while for the Pt densities the LanL2DZ BS was used.
The Gaussian09 program was used for this procedure [7]. From this conformation the RESP partial charges [8] of Pt-PyAG were carried out. The Van Der Waals (VdW) parameters of the Pt atom were those of [9], while those of the other atoms were taken from GAFF. The calculation of bonded parameters (stretching and bending force constants) of the metal coordinations were based on the Hessian matrix, using the Seminario's method [10]. Torsion force constants were set to 0 as in ref. [3].

The AA models for the various solvents, ACN and TCE, were obtained accordingly.

Coarse Grained parameters *.itp* GROMACS file format

Here below we report the .itp file (GROMACS format – energies in kJ mol^{-1}) for the developed CG models used in this work. The SCX CG beads in the Pt-PyAG cores are *de facto* SC5 MARTINI beads, where the interactions SCX-SCX has been optimized to ε = 2.0 kj/mol (instead of 2.625 kj/mol for the original SC5-SC5) in order to reproduce the AA free energy profile of the core-core interaction, obtained by means of metadynamics simulations (Figure S18).

CG model for the **Pt-PyAG** monomer:

```
Pt-PyAG
[ moleculetype ]
;name   nrexcl
 TRMR  2


[ atoms ]
;nr   type   resi   res   atom   cgnr   charge
 1  SCX  1  HEA  C1  1  0.0
 2  SCX  1  HEA  C2  2  0.0
 3  SCX  1  HEA  C3  3  0.0
 4  SCX  1  HEA  C4  4  0.0
 5  SN0  1  HEA  N1  5  0.0
 6  C2  1  HEA  P1  6  0.0
 7  SCX  1  HEA  C6  7  0.0
 8  SN0  1  HEA  N2  8  0.0
 9  C2  1  HEA  P2  9  0.0
 10  SN0  1  Pt0  Pt  10  0.0
 11  SCX  1  TAI  C7  11  0.0
 12  SCX  1  TAI  C8  12  0.0
 13  P1  1  TAI  O1  13  0.0
 14  P4  1  TAI  O2  14  0.0
 15  P5  1  TAI  O3  15  0.0
 16  EO  1  TAI  O4  16  0.0


[ constraints ]
;
[ bonds ]
;ai   aj   funct   r   k
 1  2  1  0.18  25000.00
 1  3  1  0.18  25000.00
 2  4  1  0.27  25000.00
 3  7  1  0.27  25000.00
 4  5  1  0.17  25000.00
 7  8  1  0.17  25000.00
 4  6  1  0.28  25000.00
 7  9  1  0.28  25000.00
 12  13  1  0.24  25000.00
 11  13  1  0.24  25000.00
```

```
 3  10  1  0.30  25000.00
 2  10  1  0.30  25000.00
 5  10  1  0.27  25000.00
 8  10  1  0.27  25000.00
 10  11  1  0.30  16560.28
 10  12  1  0.30  16560.28
 2  3  1  0.17  25000.00
 11  12  1  0.17  25000.00
 13  14  1  0.41  14412.18

 14  15  1  0.37  6616.01
 15  16  1  0.30  7678.43


[ angles ]
;ai   aj   ak   funct   theta   cth
 3  2  4  2  154.63  2000.00
 2  3  7  2  154.63  2000.00
 1  2  4  2  140.99  2000.00
 1  3  7  2  140.99  2000.00
 1  2  10  2  134.32  2000.00
 1  3  10  2  134.32  2000.00
 4  2  10  2  82.96  2000.00
 7  3  10  2  82.96  2000.00
 2  4  5  2  91.50  2000.00
 3  7  8  2  91.50  2000.00
 2  4  6  2  167.03  283.17
 3  7  9  2  167.03  283.17
 5  4  6  2  95.80  1988.74
 8  7  9  2  95.80  1988.74
 4  5  10  2  114.89  1634.55
 7  8  10  2  114.89  1634.55
 5  10  3  2  102.49  2000.00
 8  10  2  2  102.49  2000.00
 8  10  3  2  69.15  2000.00
 5  10  2  2  69.15  2000.00
 3  10  11  2  206.55  475.52
 3  10  12  2  206.55  475.52
 2  10  11  2  206.55  475.52
 2  10  12  2  206.55  475.52
 5  10  11  2  93.77  40.07
 5  10  12  2  93.77  40.07
 8  10  11  2  93.77  40.07
 8  10  12  2  93.77  40.07
 10  11  13  2  138.23  704.92
 10  12  13  2  138.23  704.92
 12  13  14  2  151.70  16.48
 11  13  14  2  151.70  16.48
 8  10  5  2  167.95  426.01
 13  14  15  2  93.74  38.87
 14  15  16  2  134.15  41.44
```

```
[ dihedrals ]
;i  j  k  l  func  phase  kd  pn
 4  2  3  7  9  0.49  4.89  1
 4  2  3  7  9  -177.73  2.17  2
 3  2  4  5  9  179.56  0.53  4
 3  2  4  6  9  -6.50  0.38  1
 1  2  4  5  9  -177.35  0.64  6
 1  2  4  6  9  177.50  0.46  2
 10  2  4  5  9  -0.42  5.00  1
 10  2  4  5  9  179.12  1.33  2
 10  2  4  6  9  176.11  0.50  2
 2  3  7  8  9  -178.24  0.50  4
 2  3  7  9  9  -9.01  0.36  1
 1  3  7  8  9  173.11  0.60  6
 1  3  7  9  9  174.24  0.46  2
 10  3  7  8  9  0.21  5.00  1
 10  3  7  8  9  -179.63  1.33  2
 10  3  7  9  9  170.59  0.52  2
 2  4  5  10  9  1.00  5.00  1
 2  4  5  10  9  -177.94  1.36  2
 6  4  5  10  9  6.32  0.60  5
 3  7  8  10  9  -0.87  5.00  1
 3  7  8  10  9  178.31  1.35  2
 9  7  8  10  9  0.99  0.60  5
 10  12  13  14  9  -164.54  0.27  2
 10  11  13  14  9  170.45  0.31  2
 12  13  14  15  9  -110.75  0.46  1
 12  13  14  15  9  -51.54  0.21  2
 11  13  14  15  9  -116.46  0.47  1
 11  13  14  15  9  -66.95  0.24  2
 13  14  15  16  9  -3.16  0.14  1
 13  14  15  16  9  -11.97  0.18  2
 1  3  10  5  9  178.79  0.64  6
 1  3  10  8  9  -179.00  5.00  1
 1  3  10  8  9  -177.96  1.37  2
 1  3  10  11  9  -23.36  0.10  2
 1  3  10  12  9  -35.02  0.14  3
 7  3  10  5  9  -179.82  5.00  1
 7  3  10  5  9  -179.63  1.36  2
 7  3  10  8  9  -0.04  5.00  1
 7  3  10  8  9  179.93  1.29  2
 7  3  10  11  9  -22.45  0.08  1
 7  3  10  11  9  -39.53  0.06  2
 7  3  10  12  9  12.23  0.19  6
 1  2  10  5  9  -179.73  5.00  1
 1  2  10  5  9  -179.49  1.38  2
 1  2  10  8  9  -179.90  0.69  6
 1  2  10  11  9  177.41  0.12  5
 1  2  10  12  9  -164.09  0.13  5
 4  2  10  5  9  0.32  5.00  1
 4  2  10  5  9  -179.35  1.29  2
```

```
 4  2  10  8  9  -179.87  5.00  1
 4  2  10  8  9  -179.73  1.36  2
 4  2  10  11  9  168.93  0.11  3
 4  2  10  12  9  122.41  0.15  3
 4  5  10  3  9  -0.59  5.00  1
 4  5  10  3  9  178.76  1.41  2
 4  5  10  2  9  -0.88  5.00  1
 4  5  10  2  9  178.18  1.35  2
 4  5  10  8  9  179.50  0.66  2
 4  5  10  11  9  -20.33  0.29  5
 4  5  10  12  9  7.84  0.32  5
 7  8  10  3  9  0.54  5.00  1
 7  8  10  3  9  -178.97  1.34  2
 7  8  10  2  9  0.66  5.00  1
 7  8  10  2  9  -178.69  1.41  2
 7  8  10  5  9  179.97  0.67  2
 7  8  10  11  9  3.22  0.35  5
 7  8  10  12  9  -2.56  0.31  5
 3  10  11  13  9  143.46  0.13  1
 2  10  11  13  9  -43.30  0.15  3
 5  10  11  13  9  159.69  0.21  2
 8  10  11  13  9  154.99  0.21  2
 3  10  12  13  9  -7.90  0.12  3
 2  10  12  13  9  154.90  0.14  5
 5  10  12  13  9  173.27  0.20  2
 8  10  12  13  9  -179.39  0.20  2
```

CG model for different solvents:

All solvents have been parametrized in order to respect the overall polarity, and polarity anisotropic/isotropic features, of the native solvent molecules, which is particularly important in this case. OCT has been parametrized, as in standard MARTINI, using C1 beads. TCE molecules has been parametrized as two C4 MARTINI beads. ACN has been parametrized as one SC1 and one SP4 beads (while this gives rise to ACN CG molecules that are slightly larger than the AA ones, this was necessary to respect the key polarity features of ACN, possessing a hydrophobic tail and a hydrophilic head, which can interact with the amino acid tails of the monomers).

TCE

```
[moleculetype]
; molname       nrexcl
  TCE           1

[atoms]
; id    type    resnr   residu  atom    cgnr    charge
  1     C4      1       TCE     CX      1       0
  2     C4      1       TCE     CX      2       0

[bonds]
; i j   funct   length  force.c.
  1 2   1       0.47    1250
```

ACN

```
[moleculetype]
; molname       nrexcl
  ACN           1

[atoms]
; id    type    resnr   residu  atom    cgnr    charge
  1     SP4     1       ACN     P1      1       0
  2     SC1     1       ACN     C1      2       0

[constraints]
; i j   funct   length
  1 2   1       0.27
```

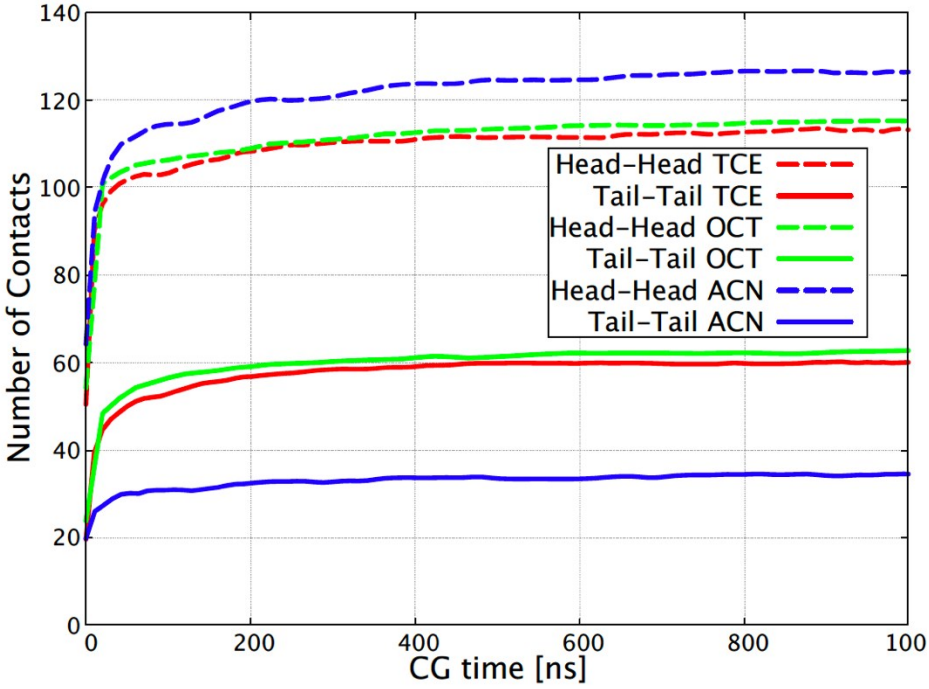

Figure S18: Number of contacts between the monomers Pt-heads (head-head) and between the peptide tails (tail-tail) in TCE, OCT and ACN obtained from CG-MD self-assembling simulations. The results show that the interactions between the monomers heads are relatively stronger in ACN than in TCE and OCT. On the contrary, the tail-tail interactions are stronger in TCE and OCT than in ACN.

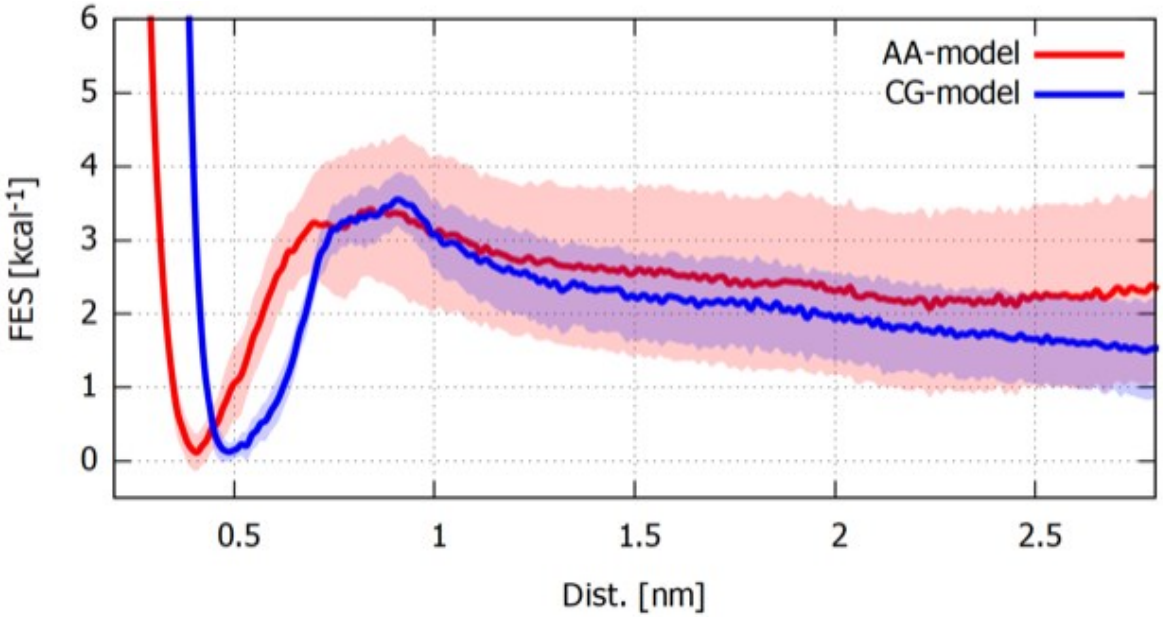

Figure S19: Free energy profile of head-head interaction obtained from AA and CG metadynamics simulations, showing consistent head-head stacking strength, and used to parametrize consistent CG models for the monomers.

References:

(1)Wang, J.; Wolf, R. M.; Caldwell, J. W.; Kollman, P. A.; Case, D. A. *J. Comput. Chem.* **2004**, *25*, 1157.
(2)Wang, J.; Wang, W.; Kollman, P. A.; Case, D. A. *Journal of Molecular Graphics and Modelling* **2006**, *25*, 247.
(3)Li, P. F.; Merz, K. M. *J. Chem Inf. Model.* **2016**, *56*, 599.
(4)Stewart, J. J. P. *J Mol Model* **2007**, *13*, 1173.
(5)Xia, Y.; Wang, X.; Zhang, Y.; Luo, B. *Computational and Theoretical Chemistry* **2011**, *967*, 213.
(6)Becke, A. D. *J. Chem. Phys.* **1993**, *98*, 5648.
(7)M. J. Frisch; G. W. Trucks; H. B. Schlegel; G. E. Scuseria; M. A. Robb; J. R. Cheeseman; G. Scalmani; V. Barone; B. Mennucci; G. A. Petersson; H. Nakatsuji; M. Caricato; X. Li; H. P. Hratchian; A. F. Izmaylov; J. Bloino; G. Zheng; J. L. Sonnenberg; M. Hada, M.; Ehara, K.; Toyota, R.; Fukuda; J. Hasegawa; M. Ishida; T. Nakajima; Y. Honda; O. Kitao; H. Nakai; T. Vreven; J. A. Montgomery; Jr., J. E. P.; F. Ogliaro; M. Bearpark; J. J. Heyd; E. Brothers; K. N. Kudin; V. N. Staroverov; R. Kobayashi; J. Normand; K. Raghavachari; A. Rendell; J. C. Burant; S. S. Iyengar; J. Tomasi; M. Cossi; N. Rega; J. M. Millam; M. Klene; J. E. Knox; J. B. Cross; V. Bakken; C. Adamo; J. Jaramillo; R. Gomperts; R. E. Stratmann; O. Yazyev; A. J. Austin; R. Cammi; C. Pomelli; J. W. Ochterski; R. L. Martin; K. Morokuma; V. G. Zakrzewski; G. A. Voth; P. Salvador; J. J. Dannenberg; S. Dapprich; A. D. Daniels; Ö. Farkas; J. B. Foresman; J. V. Ortiz; J. Cioslowski; Fox, a. D. J. *Gaussian 09, Revision E.01*, 2009.
(8)Bayly, C. I.; Cieplak, P.; Cornell, W.; Kollman, P. A. *The Journal of Physical Chemistry* **1993**, *97*, 10269.
(9)Hambley, T. W. *Inorganic Chemistry* **1998**, *37*, 3767.
(10)Seminario, J. M. International Journal of Quantum Chemistry **1996**, 60, 1271.